Prostaglandin E1 Attenuates Post-Cardiac Arrest Myocardial Dysfunction via Inhibiting Mitochondria-Mediated Cardiomyocyte Apoptosis

Chenglei Su
Shandong University
Xinhui Fan
Shandong University
Feng Xu
Shandong University
Jiali Wang (wangjiali_2000@126.com)
Shandong University https://orcid.org/0000-0002-2934-4582
Yuguo Chen
Shandong University

Research article

Keywords: prostaglandin E1, cardiac arrest, post-cardiac arrest myocardial dysfunction, mitochondrial permeability transition pore, GSK3β

Posted Date: April 13th, 2020

DOI: https://doi.org/10.21203/rs.3.rs-21943/v1

Abstract

Background: Post-cardiac arrest myocardial dysfunction (PAMD) is a leading cause of death in resuscitated patients after cardiac arrest (CA). Prostaglandin E1 (PGE1) is a clinical drug used to mitigate ischemia injury. However, its effect on PAMD remains unknown.

Methods: We investigated the protective effects of PGE1 on PAMD in a rat model of cardiac arrest and a hypoxia-reoxygenation (H/R) H9c2 cell model. Forty-two male Wistar rats were randomly assigned to CA, CA+PGE1, and sham groups. Asphyxia for 8 min followed by cardiopulmonary resuscitation was performed in the CA and CA+PGE1 groups. PGE1 (1 μg/kg) was intravenously administered at the onset of return of spontaneous circulation (ROSC). Ejection fraction (EF) and cardiac output (CO) were measured at baseline, 1, 2, 3, and 4 h after ROSC; survival was monitored for 72 h. Cardiomyocyte apoptosis, mitochondrial permeability transition pore (mPTP) opening, and protein levels of glycogen synthase kinase 3β (GSK3β), cytochrome c, and cleaved caspase-3 were measured 4 h after ROSC. H9c2 cells were treated with PGE1(0.5 μM) at the start of reoxygenation. Apoptosis, mPTP opening, and protein levels of GSK3β, cytochrome c, and cleaved caspase-3 of H9c2 cells were detected.

Results: Compared to the CA group, PGE1 treatment significantly increased the EF and CO within 4 h after ROSC and improved the survival rate. It activated GSK3β, prevented mPTP opening, suppressed cytochrome c and cleaved caspase-3 expression, and reduced cardiomyocyte apoptosis in the rat model. In vitro, Changes in GSK3β, mPTP opening, cytochrome c and cleaved caspase-3 expression, and apoptosis in H9c2 cells were consistent with those in the rat model.

Conclusions: Our results indicate that PGE1 attenuates PAMD via inhibiting mitochondria-mediated cardiomyocyte apoptosis.

Background

Cardiac arrest (CA) poses a significant public health burden. Although modern cardiopulmonary resuscitation (CPR) improves the return of spontaneous circulation (ROSC) rate in patients who suffered from CA, the outcome remains poor (Andersen *et al*, 2019; Neumar, 2016). Significant left ventricular systolic and diastolic dysfunction early after ROSC, termed post-cardiac arrest myocardial dysfunction (PAMD), is common (Jentzer *et al*, 2016). Although PAMD is temporary after resuscitation, approximately two-thirds of the patients that achieve ROSC die from PAMD within the first 72 h (Dragancea *et al*, 2013; Gonzalez *et al*, 2008; Gupta *et al*, 2019; Jentzer et al, 2015; Laurent et al, 2002; Ruiz-Bailen *et al*, 2005). Currently, pharmacological treatments to attenuate PAMD are not available (Chonde et al, 2019; Jentzer et al., 2015).

Mitochondria-mediated cardiomyocyte apoptosis is one of the primary mechanisms underlying PAMD due to CA (Heusch *et al*, 2010; Jentzer et al., 2015; Liu *et al*, 2018). Global myocardial ischemia due to CA induces mitochondrial permeability transition pore (mPTP) opening, which results in cytochrome c leaking from the mitochondrial matrix to the cytoplasm, leading to caspase-3 activation and apoptosis

(Morciano *et al*, 2017; SileikyteandForte, 2019; Wu et al, 2018). Inhibiting mPTP opening and apoptosis is a potential therapeutic target for PAMD (Cour *et al*, 2011; Huang *et al*, 2011).

Prostaglandin E1 (PGE1), an essential member of the prostaglandin family, has many physiological and pharmacological activities. PGE1 is widely used in clinic for the treatment of ischemia injury (HewandGerriets, 2019; Schutte *et al*, 2001; Weiss *et al*, 2002). PGE1 decreases mPTP opening and apoptosis in animal models of myocardial infarction and coronary microembolization (Johnson, 2000; Schutte *et al*., 2001; Zhu *et al*, 2017). However, the protective effects of PGE1 on PAMD have not been reported.

In the present study, we hypothesized that PGE1 treatment can attenuate PAMD and improve survival rates in a rat model of CA. In addition, we tested the hypothesis that PGE1 exerts cardioprotective effects by inhibiting mitochondria-mediated cardiomyocyte apoptosis.

Methods

Animals

Male Wistar rats weighing 380–430 g were purchased from the Department of Experimental Animals of Shandong University. The rats were housed in independent ventilation cages at an ambient temperature of 23 ± 1 °C and a humidity of 55 ± 5% under a 12-h light/dark cycle. They were allowed access to food and tap water *ad libitum*.

Asphyxia-induced CA model establishment and treatments

Rats were anesthetized with 5% isoflurane in room air (21% oxygen) in a plastic induction box. The trachea was orally intubated. The rats were mechanically ventilated and maintained under anesthesia with 2% isoflurane. A PE-50 catheter was advanced through the left femoral artery into the aorta for measurement of the mean aortic pressure (MAP). A microcatheter was inserted into the left femoral vein for drug administration. A conventional lead II electrocardiogram (ECG) was continuously recorded. Pancuronium-bromide (2 mg/kg) was intravenously administered for complete muscle relaxation. After pancuronium-bromide administration, the rats were administered 0.5% isoflurane in room air (21% oxygen) for 5 min.

Rats were randomly allocated to three groups (Fig. 1): (i) CA+PGE1 group: rats underwent 8 min of asphyxia followed by CPR, and lipo-PGE1 (1 μg/kg, purchased from Qilu Pharmaceutical, Jinan, China) was intravenously administered at the onset of ROSC (Fang *et al*, 2010; Zhu *et al*., 2017); (ii) CA group: rats underwent 8 min of asphyxia and CPR; and (iii) sham group: rats underwent the same surgical procedure without asphyxia or CPR. The rat model of asphyxia-induced CA was established as described previously (Kim *et al*, 2016; Wei *et al*, 2019). After Pancuronium-bromide administration, the rats were administered 0.5% isoflurane in room air (21% oxygen) for 5 min. CA was induced by asphyxia, which occurred after turning off the ventilator and clamping the endotracheal tube. The hypotension and

heart rate dropped quickly. Cardiac arrest was defined as a MAP of <20 mmHg. After 8 min of asphyxia, chest compression was started at a rate of 200 beats/min. The MAP was maintained at >25 mmHg during resuscitation. Mechanical ventilation with 100% oxygen and a bolus injection of epinephrine (10 μg/kg) via a venous line were initiated 30 s before chest compression. Chest compressions were continued, and epinephrine was injected every 5 min until ROSC was achieved. ROSC was defined as the return of supraventricular rhythm with an increase in mean artery pressure of more than 50 mmHg for 5 min. Only rats that achieved ROSC within 10 min (n = 42) were used for further study. At 4 h after ROSC, 21 rats (n = 7/group) were sacrificed and the hearts were collected. The remaining 21 rats were used for 72-h survival analysis.

Cardiac function monitoring

Cardiac function was measured using an ultra-high frequency ultrasound system for small animals (Vevo 2100; Visual Sonics, Toronto, Canada). Left ventricular end-diastolic diameter (LVEDD), left ventricular end-systolic diameter (LVESD), left ventricular end-diastolic volume (LVEDV), left ventricular end-systolic volume (LVESV) and heart rate (HR) were recorded from M-mode images. Ejection fraction (EF) and cardiac output (CO) were calculated as follows: EF = (LVEDV−LVESV)/LVEDV ×l00%; CO = (LVEDV−LVESV) × HR. All measurements were reviewed and confirmed separately by two investigators.

Survival analysis

For the 72-h survival study, all catheters were removed and wounds were surgically closed at 4 h after ROSC. The rats were then returned to their cages and closely monitored during 72 h.

Hypoxia-reoxygenation (H/R) cell model establishment

Rat cardiomyoblasts (H9c2) were obtained from the Cell Bank of the Chinese Academy of Sciences (Shanghai, China) and were grown in high-glucose DMEM supplemented with 10% fetal bovine serum and 1% penicillin/streptomycin at 37°C in an atmosphere of 5% CO_2 in air.

H/R procedures were performed as described previously (Huang *et al*, 2016; Pu *et al*, 2019). Briefly, H9c2 cells in no-glucose DMEM were exposed to 1% O_2, 94% N_2, and 5% CO_2 in an anaerobic glove box (Don Whitley Scientific, Bingley, UK) for 12 h to mimic ischemia. Then, the medium was replaced with high-glucose DMEM and the cells were transferred to a regular incubator (95% air, 5% CO_2, 37°C) for 12 h to mimic reperfusion. H9c2 cells were treated with PGE1 (0.5 μM) at the start of reoxygenation.

Terminal deoxynucleotide nick-end labeling (TUNEL) assay

Cardiomyocyte apoptosis in rats was detected by a TUNEL assay using an In Situ Apoptosis Detection Kit (Millipore, MA, USA) according to the manufacturer's instructions. Heart tissue sections were stained with 3-3¢-diaminobenzidine to detect TUNEL-positive cells, then counter-stained with methyl-green and examined with light microscopy (Olympus BX41, Tokyo, Japan).

H9c2 cell apoptosis was detected by a TUNEL assay using an Apoptosis Assay Kit (Roche, CA, USA) per the manufacturer's instructions. After TUNEL staining and DAPI staining, the cells were imaged under a fluorescence microscope (Olympus IX73, Tokyo, Japan) using 540-nm excitation and 580-nm emission. Cells exhibiting red fluorescence were defined as TUNEL-positive, apoptotic cells.

The levels of apoptosis were calculated by counting TUNEL-positive myocyte nuclei in three randomly selected fields (400×) in each slide. The levels were reported as a percentage of total myocyte nuclei.

Measurement of mPTP opening

Mitochondria of rat myocardium or H9c2 cells were isolated by differential centrifugation using a Tissue/Cell Mitochondria Isolation Kit (Beyotime, Beijing, China) according to the manufacturer's instructions. Fresh mitochondria were used for the measurement of mPTP opening, and the rest components (cytoplasmic protein without mitochondria) were used for the measurement of cytochrome c.

mPTP opening was measured using a Purified Mitochondrial Membrane Pore Channel Colorimetric Assay kit (Genmed, Shanghai, China). mPTP opening causes mitochondrial swelling, which results in a reduction of the absorbance at 520 nm (A_{520}). Changes in A_{520} at various time points were measured for each sample. The value at −1 min normalized to the value at 10 min was used for statistical analysis.

For H9c2 cells, we used an additional immunofluorescence method to measure mPTP opening. In brief, cells were washed with phosphate-buffered saline and then stained with 1 μmol/l calcein-AM (Invitrogen, Eugene, OR, USA) in the presence of 8 mmol/l $CoCl_2$ (Sigma, MO, USA) at room temperature for 20 min in the dark. $CoCl_2$ was added to quench the cytoplasmic signal so that only fluorescence in the mitochondria was captured. A change in fluorescence intensity is an index of mPTP opening.

Western blotting analysis

Total protein was extracted from heart tissues and H9c2 cells. Total protein was used to measure the expression of GSK3β and cleaved-caspase3. Cytoplasmic protein without mitochondria was used to measure cytochrome c expression. Samples with equal amounts of protein (50ug) were loaded onto 10% sodium dodecyl sulfate–polyacrylamide gels, subjected to electrophoresis and subsequently blotted onto 0.22 μM polyvinylidene fluoride (PVDF) membranes (Millipore, USA). After blocking with 5% nonfat milk, the membranes were incubated with the following primary antibodies: anti-total GSK3β (#12456, Cell Signaling Technology, USA), anti-phospho-GSK3β (Ser9, #55558, Cell Signaling Technology), anti-cleaved caspase-3 (#9664, Cell Signaling Technology, USA), anti-cytochrome c (#11940, Cell Signaling Technology, USA). Anti-β-actin (60008-1, Proteintech, China) was used to detect reference protein expression. Relative band intensities were quantified using the ImageJ software.

Statistical analysis

Data are expressed as the mean ± SD of at least three independent experiments.

Group comparisons were performed by one-way analysis of variances (ANOVA) with Tukey's post hoc test or Student's t-test. Comparisons between time-based measurements within each group were performed by repeated-measures ANOVA.

Survival analyses were conducted based on Kaplan–Meier plots and log-rank tests. Two-sided *P*-values less than 0.05 were considered statistically significant. Statistical analyses were performed using GraphPad Prism 7.0.

Results

Baseline characteristics of rats and resuscitation characteristics

In total, 42 rats were used in the present study. There were no significant differences in body weight, baseline MAP, and heart rate between the treatment groups ($P > 0.05$, Table 1). There were no significant differences in the duration of CA, epinephrine dose, duration of CPR, MAP, and heart rate at 1 h after ROSC between the CA group and the CA + PGE1 group ($P > 0.05$, Table 1). There were no significant differences in baseline cardiac function between the groups ($P > 0.05$, Fig. 2).

Table 1
Baseline characteristics of rats and resuscitation characteristics.

	CA(n = 14)	CA + PGE1(n = 14)	Sham(n = 14)
Body weight(g)	400.7 ± 17.8	411.4 ± 14.7	413.5 ± 10.1
Heart rate(bpm) before asphyxia	357.2 ± 33.4	363.5 ± 45.6	340.8 ± 29.9
MAP (mmHg) before asphyxia	133.7 ± 15.6	131.8 ± 18.9	137.3 ± 10.1
MAP (mmHg) at 1 h after ROSC	96.2 ± 15.2	94 ± 17.83	-
Cardiac arrest time(s)	274.9 ± 37.2	271.1 ± 29.8	-
CPR duration(s)	43.0 ± 12.1	43.7 ± 16.5	-
Adrenaline dose(μg)	4.1 ± 0.2	4.1 ± 0.2	-
MAP: mean aortic pressure. CPR: cardiopulmonary resuscitation			

PGE1 ameliorates cardiac dysfunction

As shown in Figure 2, CO and EF were measured in the three treatment groups at baseline and 1, 2, 3, and 4 h after ROSC. The results showed that CO and EF were significantly impaired within 4 h after ROSC in the CA group when compared to the sham group, but were significantly preserved by PGE1 treatment ($P < 0.05$, Fig. 2). When comparing the mean EF values between the CA and CA+PGE1 groups, we found a more significant difference at 4 h after ROSC (65.8 % ± 16.2 % *vs.* 81.2 % ± 9.91 %, $P < 0.01$, Fig. 2B).

PGE1 improves the survival rate

Survival statuses were followed up for 72 h. Kaplan–Meier survival curves revealed a rapid decline in the survival rate in the CA group within 24 h after ROSC (Fig. 3). The survival rate in the CA+PGE1 group was significantly higher than that in the CA group ($P < 0.01$, Fig. 3).

PGE1 suppresses cardiomyocyte apoptosis

Myocardial apoptosis was detected by TUNEL staining. *In vivo*, the level of apoptosis in the CA group was significantly increased when compared to that in the sham group (12.11 ± 4.37% vs. 48.33 ± 19.07%, $P < 0.05$, Fig. 4A). In contrast, cardiac apoptosis decreased after treatment with PGE1 (48.33 ± 19.07 vs. 31.02 ± 13.51%, $P < 0.05$, Fig. 4A). *In vitro*, the fraction of apoptotic H9c2 cells was significantly higher in the in H/R group than in the control group (6.38 ± 2.02 vs. 52.13 ± 7.86%, $P < 0.01$, Fig. 4B). The fraction of apoptotic H9c2 cells in the H/R+PGE1 group was significantly smaller than that in the H/R group (52.13 ± 7.86% vs. 31.20% ± 12.62, $P < 0.01$, Fig. 4B).

PGE1 blocks mPTP opening

In vivo, the mitochondrial swelling rate after exposure to $CaCl_2$ was increased in the CA group compared to the sham group (0.61 ± 0.11 vs. 0.82 ± 0.13, $P < 0.05$, Fig. 5C, D). PGE1 treatment reduced mPTP opening (0.76 ± 0.11 vs. 0.61 ± 0.12 in the CA group, $P < 0.05$, Fig. 5C, D). *In vitro*, mPTP opening was blocked by PGE1 treatment (0.58 ± 0.10 vs. 0.77 ± 0.13 in the H/R group, $P < 0.05$, Fig. 5A, B). Consistent with the mitochondrial swelling assay results, the relative fluorescence intensity of calcein AM was significantly higher in the H/R+PGE1 group than in the H/R group (0.41 ± 0.12 vs. 0.72 ± 0.24, $P < 0.01$, Fig. 5E–H).

PGE1 regulates cytochrome c, caspase 3, and GSK3β

In vivo, the protein levels of cytochrome c (cytoplasmic) and cleaved caspase-3 were significantly increased in the CA group as compared to the levels in the sham group ($P < 0.01$, Fig. 6A). PGE1 treatment partially suppressed these increases ($P < 0.01$, Fig. 6B). *In vitro*, consistent results were obtained. PGE1 treatment alleviated the increase in cytochrome c (cytoplasmic) and cleaved caspase-3 induced by H/R ($P < 0.01$, Fig. 6B).

To evaluate the upstream pathway, GSK3β protein phosphorylation was analyzed. *In vivo*, GSK3β phosphorylation was decreased in the CA group compared to the sham group ($P < 0.01$, Fig. 6A). GSK3β phosphorylation was higher in the CA+PGE1 than in the CA group ($P < 0.01$, Fig. 6A). *In vitro*, GSK3β phosphorylation was decreased in the H/R group ($P < 0.01$), but was partly restored by PGE1 treatment ($P < 0.01$, Fig. 6B).

Discussion

PAMD is common and worsens survival in resuscitated patients after CA. There are currently no effective strategies for PAMD (Jentzer et al., 2015; Kang, 2019). In the present study, we found that PGE1 treatment

improved cardiac function and the survival outcome after ROSC in a rat model of CA induced by asphyxia. Moreover, based on *in vitro* experiments, we found that inhibition of mitochondria-mediated cardiomyocyte apoptosis is involved in the mechanism underlying the protective effect of PGE1.

The rat model of asphyxia-induced CA used in the present study is a common animal model for CA (Vognsen *et al*, 2017). We measured the EF and CO in the experimental animals, which confirmed a significant impairment of cardiac function after CA. Interestingly, PGE1 treatment attenuated cardiac dysfunction as of 1 h after ROSC. Further, PGE1 significantly improved the EF at 4 h after ROSC. These results indicated that PGE1 has protective effects against PAMD.

The underlying mechanism was investigated in the *in-vivo* and *in-vitro* models. The primary causes of PAMD are myocardial apoptosis and stunning following ischemia-reperfusion injury (Jentzer et al., 2015; Piao et al, 2019). Inhibiting apoptosis can effectively alleviate organ disorders (Zhao et al, 2019). Gu et al. (Gu *et al*, 2012) reported that inhibition of cardiomyocyte apoptosis can improve cardiac function after CA. In the present study, we focused on cardiomyocyte apoptosis after CA. Our results indicated that PGE1 treatment significantly ameliorated cardiomyocyte apoptosis after CA.

As mitochondrial disorder plays a vital role in myocardial apoptosis (Kuznetsov et al, 2019; Piao et al., 2019; Zheng *et al*, 2019; Zhou et al, 2019), we investigated mPTP opening. mPTP opening in the inner mitochondrial membrane results in collapse of the membrane potential, matrix swelling, and the release of cytochrome c into the cytoplasm, where it activates caspase-3, leading to apoptosis (Kuznetsov et al., 2019; SileikyteandForte, 2019). Growing evidence indicates that inhibition of mPTP opening is an effective treatment to reduce apoptosis in many pathological conditions (Cour *et al*., 2011; Sun *et al*, 2019; Wang *et al*, 2019). We observed increases in mPTP was after CA or H/R. However, PGE1 treatment effectively blocked the excessive mPTP opening. Similarly, Cour et al. (Cour *et al*, 2014) reported that cyclosporine A (an inhibitor of mPTP opening) attenuated post-CA syndrome and improved short-term outcomes in a rabbit model. Zhu et al. (Zhu *et al*., 2017) reported that PGE1 pretreatment prevented mPTP opening in a rat model of coronary microembolization. These findings support our hypothesis that PGE1 inhibits mPTP opening.

Cytochrome c and caspase-3 are downstream proteins in mitochondria-mediated cardiomyocyte apoptosis. When a cell is stimulated by particular pathological factors, macromolecules, including cytochrome c, procaspase-2, and procaspase-9, are released through the mPTP. Cytochrome c plays a central role in apoptosis. Once released into the cytosol, it forms a complex known as the apoptosome. These events allow for the catalytic maturation of caspase-3, which eventually mediates apoptosis (Morciano *et al*., 2017; SileikyteandForte, 2019; Wu et al., 2018). To identify the mechanism underlying the antiapoptotic effects of PGE1, we detected the protein levels of (cytosolic) cytochrome c and cleaved caspase-3. CA increased cytochrome c and cleaved caspase-3 expression in the heart, which is consistent with findings reported by Garcia et al. (Garcia *et al*, 2017). PGE1 treatment significantly attenuated the pathologic increases in cytochrome c and cleaved caspase-3 induced by CA.

To evaluate how PGE1 treatment inhibited mPTP opening, we measured the activation of GSK3β, which is a primary upstream mPTP regulator (Nikolaou *et al*, 2019; Tanaka *et al*, 2018; Yang *et al*, 2017). GSK3β (Ser9) phosphorylation was decreased after CA, but PGE1 treatment preserved the activation of GSK3β. Therefore, we speculate that PGE1 inhibits mPTP opening by activating GSK3β.

Our study had certain limitations. First of all, our CA model was induced by asphyxia. It remains unknown whether the cardioprotective effects of PGE1 are the same in CA induced by ventricular fibrillation. Second, we did not use inhibitors to further evaluate the role of the GSK3β pathway in the cardioprotective mechanism of PGE1. Third, side effects of PGE1 on hemodynamics were not fully assessed. In clinic, PGE1 has a risk of decreasing blood pressure. We stopped recording MAP at 1 h after ROSC because of technical matters. Although the MAP at 1 h after ROSC was not significantly different between the CA and CA + PGE1 groups, the safety of PGE1 remains to be further evaluated before the cardioprotective effects of PGE1 can be investigated in clinical studies.

Conclusions

In conclusion, PGE1 treatment at the onset of ROSC attenuated PAMD and improved the survival rate after CA. Its benefits were partially attributed to inhibition of mitochondria-mediated cardiomyocyte apoptosis, which likely involves the GSK3β pathway. These findings offer significant insights into developing new strategies for PAMD.

Abbreviations

PAMD
Post-cardiac arrest myocardial dysfunction PAMD
CA
cardiac arrest
PGE1
prostaglandin E1
H/R
hypoxia-reoxygenation
ROSC
return of spontaneous circulation
EF
ejection fraction
CO
cardiac output
mPTP
mitochondrial permeability transition pore
GSK3β
glycogen synthase kinase 3β

CPR
cardiopulmonary resuscitation
MAP
mean aortic pressure
ECG
electrocardiogram
LVEDD
Left ventricular end-diastolic diameter
LVESD
left ventricular end-systolic diameter
LVEDV
left ventricular end-diastolic volume
LVESV
left ventricular end-systolic volume
HR
heart rate
TUNEL
Terminal deoxynucleotide nick-end labeling
PVDF
polyvinylidene fluoride
ANOVA
one-way analysis of variances

Declarations

Ethics approval and consent to participate

Animal experiments were conducted following the guide for the Care and Use of Laboratory Animals of the National Institutes of Health (USA) and following protocols approved by the Animal Use and Care Committee of Shandong University (Jinan, China).

Consent for publication

Not applicable

Availability of data and materials

The datasets used and/or analysed during the current study are available from the corresponding author on reasonable request.

Competing interests

The authors declare that they have no competing interests

Funding

This study was supported by the National Key R&D Program of China (2017YFC0908700, 2017YFC0908703), National Natural Science Foundation of China (81772036, 81671952, 81873950, 81873953, 81570401, 81571934), National S&T Fundamental Resources Investigation Project (2018FY100600, 2018FY100602), Taishan Pandeng Scholar Program of Shandong Province (tspd20181220), Taishan Young Scholar Program of Shandong Province (tsqn20161065, tsqn201812129), Key R&D Program of Shandong Province (2016ZDJS07A14, 2018GSF118003) and the Fundamental Research Funds of Shandong University (2018JC011).

Authors' contributions

CLS and XHF performed all the animal and cell studies. FX analyzed the data. YGC and JLW designed the work and revised it.

Acknowledgements

Not applicable

References

1. Andersen LW, Holmberg MJ, Berg KM, Donnino MW, Granfeldt A.In-Hospital Cardiac Arrest: A Review. *JAMA.2019* 321: 1200–1210.
2. Chonde M, Flickinger KL, Sundermann ML, Koller AC, Salcido DD, Dezfulian C, et al.Intra-Arrest Administration of Cyclosporine and Methylprednisolone Does Not Reduce Postarrest Myocardial Dysfunction. *Biomed Res Int.2019* 2019: 6539050.
3. Cour M, Abrial M, Jahandiez V, Loufouat J, Belaidi E, Gharib A, et al.Ubiquitous protective effects of cyclosporine A in preventing cardiac arrest-induced multiple organ failure. *J Appl Physiol (1985).2014* 117: 930–936.
4. Cour M, Loufouat J, Paillard M, Augeul L, Goudable J, Ovize M, et al.Inhibition of mitochondrial permeability transition to prevent the post-cardiac arrest syndrome: a pre-clinical study. *Eur Heart J.2011* 32: 226–235.
5. Dragancea I, Rundgren M, Englund E, Friberg H, Cronberg T.The influence of induced hypothermia and delayed prognostication on the mode of death after cardiac arrest. *Resuscitation.2013* 84: 337–342.
6. Fang WT, Li HJ, Zhou LS.Protective effects of prostaglandin E1 on human umbilical vein endothelial cell injury induced by hydrogen peroxide. *Acta Pharmacol Sin.2010* 31: 485–492.
7. Garcia NA, Moncayo-Arlandi J, Vazquez A, Genoves P, Calvo CJ, Millet J, et al.Hydrogen Sulfide Improves Cardiomyocyte Function in a Cardiac Arrest Model. *Ann Transplant.2017* 22: 285–295.

8. Gonzalez MM, Berg RA, Nadkarni VM, Vianna CB, Kern KB, Timerman S, et al.Left ventricular systolic function and outcome after in-hospital cardiac arrest. *Circulation.2008* 117: 1864–1872.
9. Gu W, Li C, Yin W, Guo Z, Hou X, Zhang D.Shen-fu injection reduces postresuscitation myocardial dysfunction in a porcine model of cardiac arrest by modulating apoptosis. *Shock.2012* 38: 301–306.
10. Gupta A, Gupta A, Saba S.Change in myocardial function after resuscitated sudden cardiac arrest and its impact on long-term mortality and defibrillator implantation. *Indian Pacing Electrophysiol J.2019* 19: 150–154.
11. Heusch G, Boengler K, Schulz R.Inhibition of mitochondrial permeability transition pore opening: the Holy Grail of cardioprotection. *Basic Res Cardiol.2010* 105: 151–154.
12. Hew MR, Gerriets V. (2019) Prostaglandin E1. In: *StatPearls*, Treasure Island (FL).
13. Huang CH, Tsai MS, Hsu CY, Su YJ, Wang TD, Chang WT, et al.Post-cardiac arrest myocardial dysfunction is improved with cyclosporine treatment at onset of resuscitation but not in the reperfusion phase. *Resuscitation.2011* 82Suppl 2: S41-47.
14. Huang X, Zuo L, Lv Y, Chen C, Yang Y, Xin H, et al.Asiatic Acid Attenuates Myocardial Ischemia/Reperfusion Injury via Akt/GSK-3beta/HIF-1alpha Signaling in Rat H9c2 Cardiomyocytes. *Molecules*.2016 21.
15. Jentzer JC, Chonde MD, Dezfulian C.Myocardial Dysfunction and Shock after Cardiac Arrest. *Biomed Res Int.2015* 2015: 314796.
16. Jentzer JC, Chonde MD, Shafton A, Abu-Daya H, Chalhoub D, Althouse AD, et al.Echocardiographic left ventricular systolic dysfunction early after resuscitation from cardiac arrest does not predict mortality or vasopressor requirements. *Resuscitation.2016* 106: 58–64.
17. Johnson RG.Prostaglandin E1 and myocardial reperfusion injury. *Crit Care Med.2000* 28: 2649–2650.
18. Kang Y.Management of post-cardiac arrest syndrome. *Acute Crit Care.2019* 34: 173–178.
19. Kim T, Paine MG, Meng H, Xiaodan R, Cohen J, Jinka T, et al.Combined intra- and post-cardiac arrest hypothermic-targeted temperature management in a rat model of asphyxial cardiac arrest improves survival and neurologic outcome compared to either strategy alone. *Resuscitation.2016* 107: 94–101.
20. Kuznetsov AV, Javadov S, Margreiter R, Grimm M, Hagenbuchner J, Ausserlechner MJ.The Role of Mitochondria in the Mechanisms of Cardiac Ischemia-Reperfusion Injury. *Antioxidants (Basel*).2019 8.
21. Laurent I, Monchi M, Chiche JD, Joly LM, Spaulding C, Bourgeois B, et al. Reversible myocardial dysfunction in survivors of out-of-hospital cardiac arrest. J Am Coll Cardiol. 2002;40:2110–6.
22. Liu S, Xu J, Gao Y, Shen P, Xia S, Li Z, et al.Multi-organ protection of ulinastatin in traumatic cardiac arrest model. *World J Emerg Surg.2018* 13: 51.
23. Morciano G, Bonora M, Campo G, Aquila G, Rizzo P, Giorgi C, et al.Mechanistic Role of mPTP in Ischemia-Reperfusion Injury. *Adv Exp Med Biol.2017* 982: 169–189.

24. Neumar RW.Doubling Cardiac Arrest Survival by 2020: Achieving the American Heart Association Impact Goal. *Circulation.2016* 134: 2037–2039.
25. Nikolaou PE, Boengler K, Efentakis P, Vouvogiannopoulou K, Zoga A, Gaboriaud-Kolar N, et al.Investigating and re-evaluating the role of glycogen synthase kinase 3 beta kinase as a molecular target for cardioprotection by using novel pharmacological inhibitors. *Cardiovasc Res.2019* 115: 1228–1243.
26. Piao L, Fang YH, Hamanaka RB, Mutlu GM, Dezfulian C, Archer SL, et al.Suppression of Superoxide-Hydrogen Peroxide Production at Site IQ of Mitochondrial Complex I Attenuates Myocardial Stunning and Improves Postcardiac Arrest Outcomes. *Crit Care Med.*2019.
27. Pu Y, Wu D, Lu X, Yang L.Effects of GCN2/eIF2alpha on myocardial ischemia/hypoxia reperfusion and myocardial cells injury. *Am J Transl Res.2019* 11: 5586–5598.
28. Ruiz-Bailen M, Aguayo de Hoyos E, Ruiz-Navarro S, Diaz-Castellanos MA, Rucabado-Aguilar L, Gomez-Jimenez FJ, et al.Reversible myocardial dysfunction after cardiopulmonary resuscitation. *Resuscitation.2005* 66: 175–181.
29. Schutte H, Lockinger A, Seeger W, Grimminger F.Aerosolized PGE1, PGI2 and nitroprusside protect against vascular leakage in lung ischaemia-reperfusion. *Eur Respir J.2001* 18: 15–22.
30. Sileikyte J, Forte M.The Mitochondrial Permeability Transition in Mitochondrial Disorders. *Oxid Med Cell Longev.2019* 2019: 3403075.
31. Sun T, Ding W, Xu T, Ao X, Yu T, Li M, et al.Parkin Regulates Programmed Necrosis and Myocardial Ischemia/Reperfusion Injury by Targeting Cyclophilin-D. *Antioxid Redox Signal.2019* 31: 1177–1193.
32. Tanaka T, Saotome M, Katoh H, Satoh T, Hasan P, Ohtani H, et al.Glycogen synthase kinase-3beta opens mitochondrial permeability transition pore through mitochondrial hexokinase II dissociation. *J Physiol Sci.2018* 68: 865–871.
33. Vognsen M, Fabian-Jessing BK, Secher N, Lofgren B, Dezfulian C, Andersen LW, et al.Contemporary animal models of cardiac arrest: A systematic review. *Resuscitation.2017* 113: 115–123.
34. Wang H, Chen S, Zhang Y, Xu H, Sun H.Electroacupuncture ameliorates neuronal injury by Pink1/Parkin-mediated mitophagy clearance in cerebral ischemia-reperfusion. *Nitric Oxide.2019* 91: 23–34.
35. Wei L, Zhao W, Hu Y, Wang X, Liu X, Zhang P, et al.Exploration of the optimal dose of HOE-642 for the protection of neuronal mitochondrial function after cardiac arrest in rats. *Biomed Pharmacother.2019* 110: 818–824.
36. Weiss T, Fischer D, Hausmann D, Weiss C.Endothelial function in patients with peripheral vascular disease: influence of prostaglandin E1. *Prostaglandins Leukot Essent Fatty Acids.2002* 67: 277–281.
37. Wu HY, Huang CH, Lin YH, Wang CC, Jan TR. Cannabidiol induced apoptosis in human monocytes through mitochondrial permeability transition pore-mediated ROS production. Free Radic Biol Med. 2018;124:311–8.
38. Yang K, Chen Z, Gao J, Shi W, Li L, Jiang S, et al.The Key Roles of GSK-3beta in Regulating Mitochondrial Activity. *Cell Physiol Biochem.2017* 44: 1445–1459.

39. Zhao Z, Qu F, Liu R, Xia Y.Differential expression of miR-142-3p protects cardiomyocytes from myocardial ischemia-reperfusion via TLR4/NFkB axis. *J Cell Biochem*.2019.
40. Zheng JH, Xie L, Li N, Fu ZY, Tan XF, Tao R, et al.PD98059 protects the brain against mitochondrial-mediated apoptosis and autophagy in a cardiac arrest rat model. *Life Sci.2019* 232: 116618.
41. Zhou X, Qu Y, Gan G, Zhu S, Huang Y, Liu Y, et al.Cyclosporine A Plus Ischemic Postconditioning Improves Neurological Function in Rats After Cardiac Resuscitation. *Neurocrit Care*.2019.
42. Zhu H, Ding Y, Xu X, Li M, Fang Y, Gao B, et al.Prostaglandin E1 protects coronary microvascular function via the glycogen synthase kinase 3beta-mitochondrial permeability transition pore pathway in rat hearts subjected to sodium laurate-induced coronary microembolization. *Am J Transl Res.2017* 9: 2520–2534.

Figures

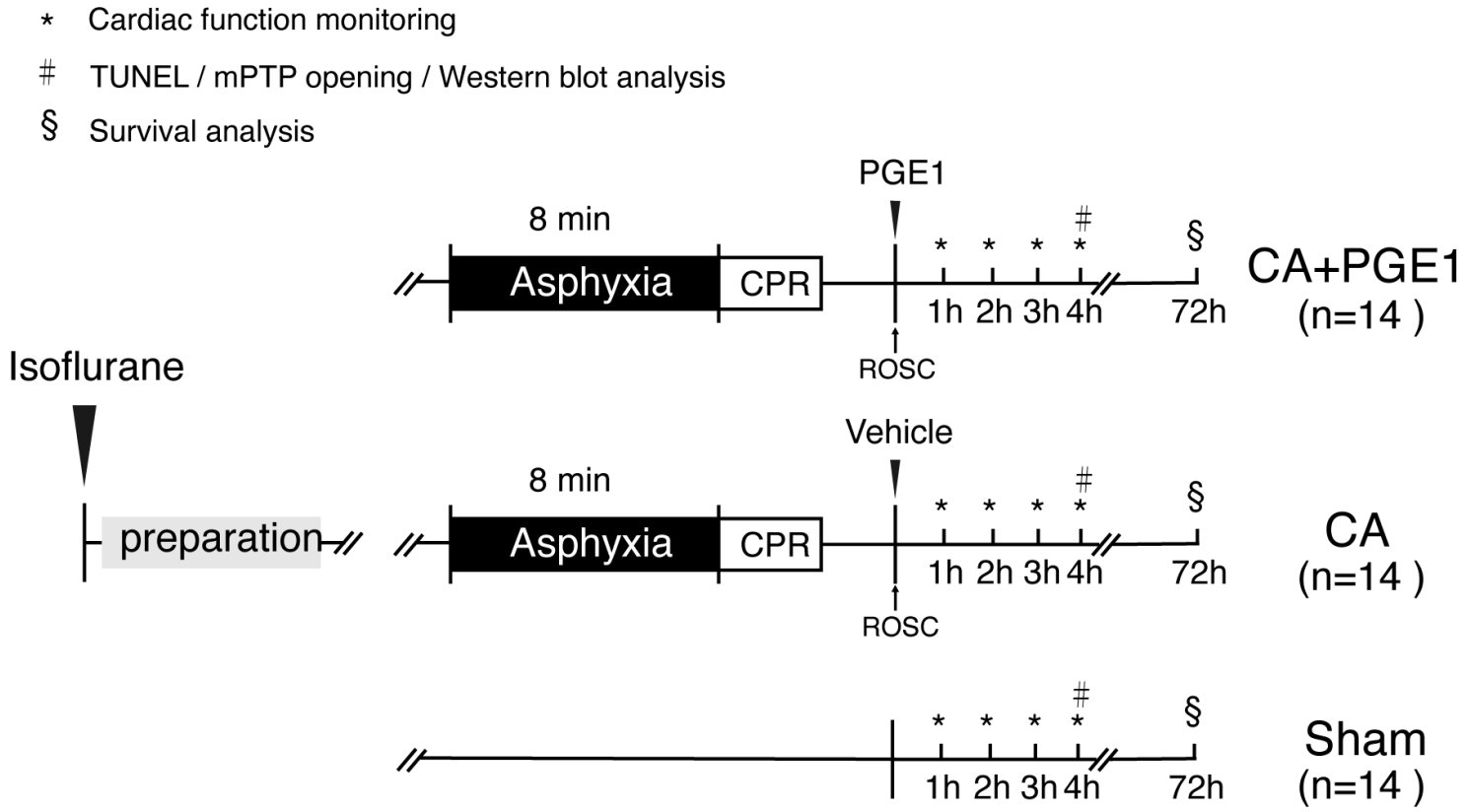

Figure 1

Experimental design of in vivo study. CA: cardiac arrest. CPR: cardiopulmonary resuscitation. ROSC: return of spontaneous circulation

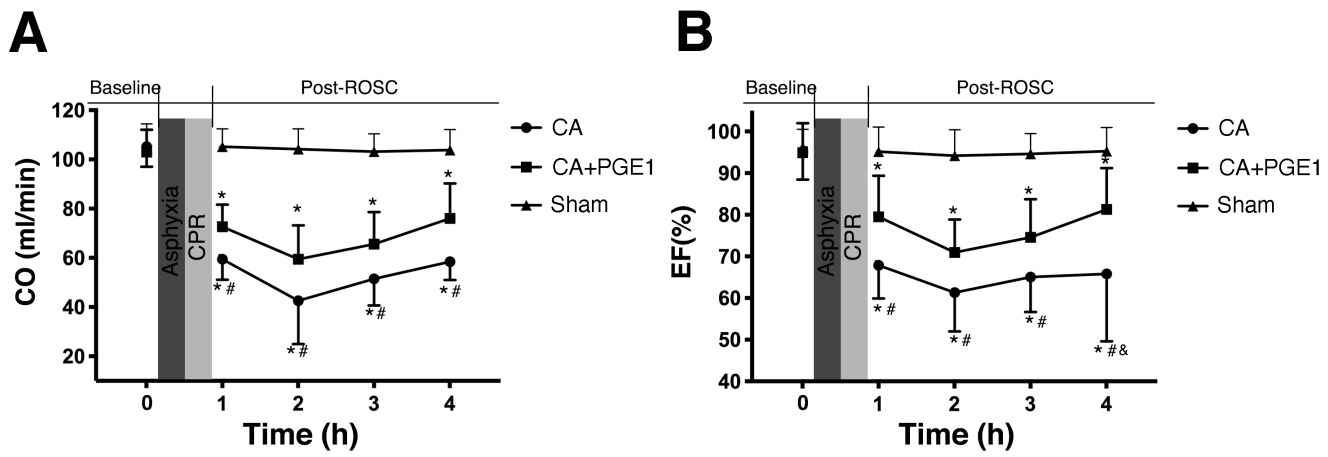

Figure 2

Changes of cardiac function. (A): Cardiac output (CO) in three groups from baseline to 4 hours after ROSC (n = 7 per each group). (B): Ejection fraction (EF) in three groups from baseline to 4 hours after ROSC (n=7 per each group). * P < 0.05, vs. sham group; # P < 0.05 vs. CA+PGE1 group; & P < 0.01 vs. CA+PGE1 group. CPR: cardiopulmonary resuscitation. ROSC: return of spontaneous circulation

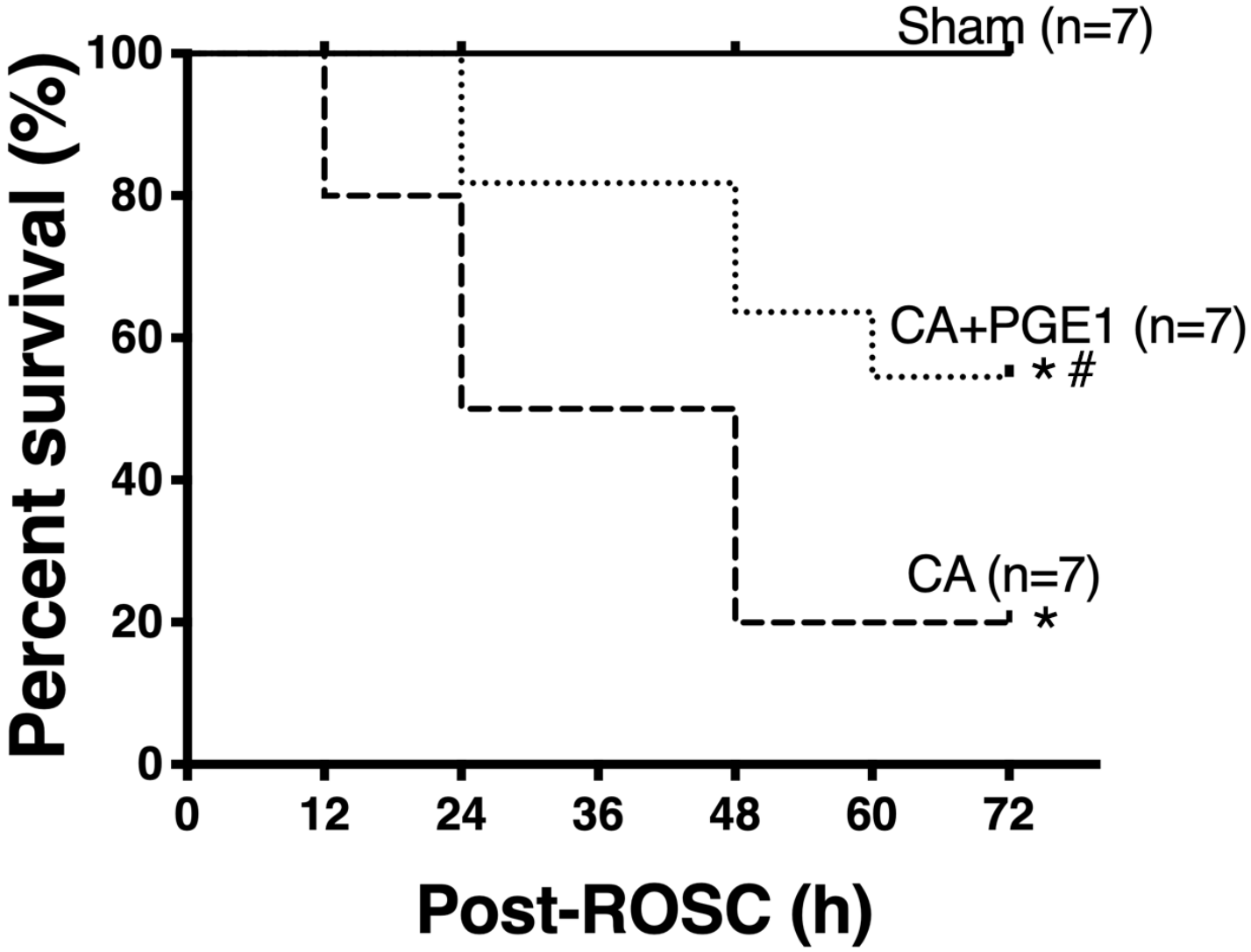

Figure 3

Survival rate during the first 72 hours after ROSC. * P < 0.01, vs. sham group; # P < 0.01, vs. CA group. ROSC: return of spontaneous circulation

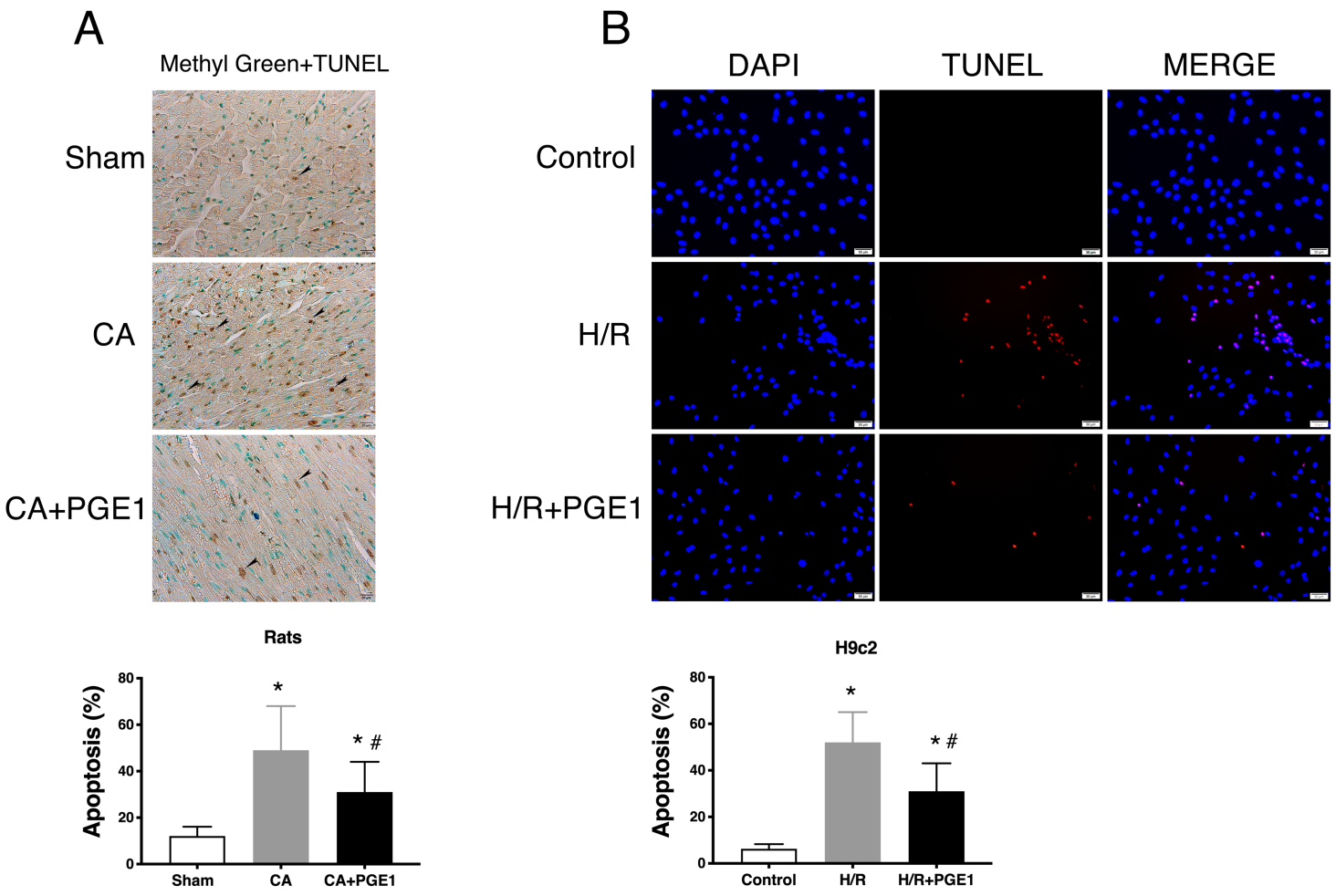

Figure 4

Apoptosis Assayed with TUNEL Staining. (A): Apoptosis analysis of rat myocardium using light microscopy. Scale bars: 20 μm. * P < 0.05 vs. Sham group, * P < 0.05 vs. control group. (B): Apoptosis analysis of H9c2 cells using fluorescent microscopy. Scale bars: 50 μm. * P < 0.01 vs. control group, # P < 0.01 vs. H/R group.

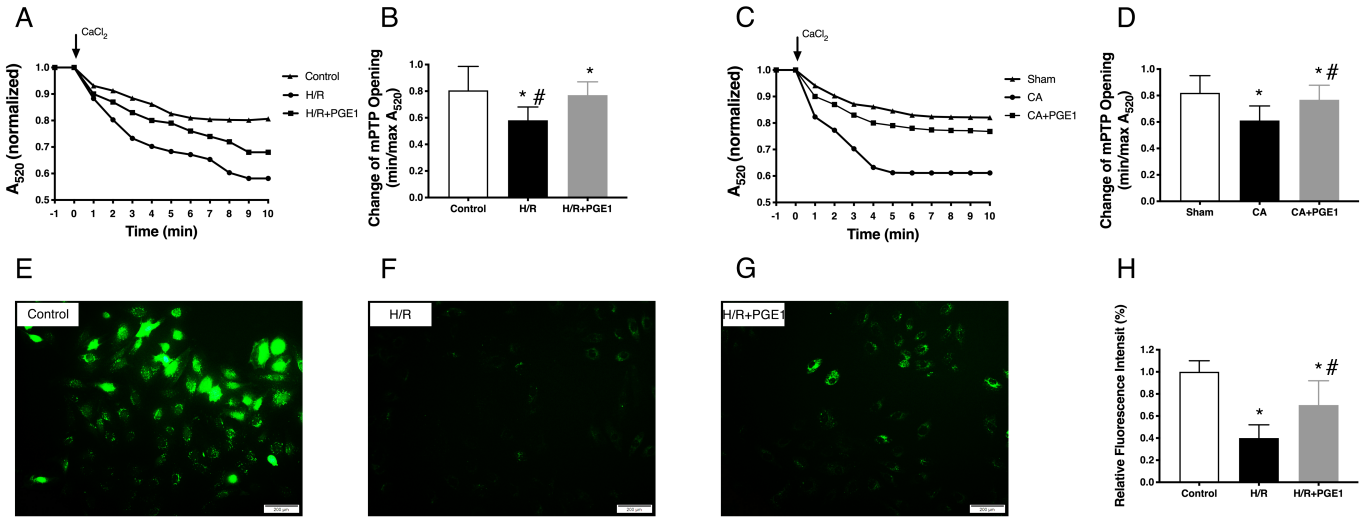

Figure 5

Effects of PGE1 on isolated mitochondrial permeability transition pore (mPTP) opening. (A, C): Downward sloping curves indicating mPTP opening induced by CaCl2 in H9c2 cells and rats. (B, D): A520 change (A520 at -1 min /A520 at 10 min) indicating mPTP opening in H9c2 cells and rats. # P < 0.05 vs. control group or sham group, * P < 0.05 vs. H/R group or CA group. (E, F, G, H): The opening of mPTP was assessed by fluorescence intensity of calcein-AM in H9c2 cells. # P < 0.01 vs. control group, * P < 0.01 vs. H/R group.

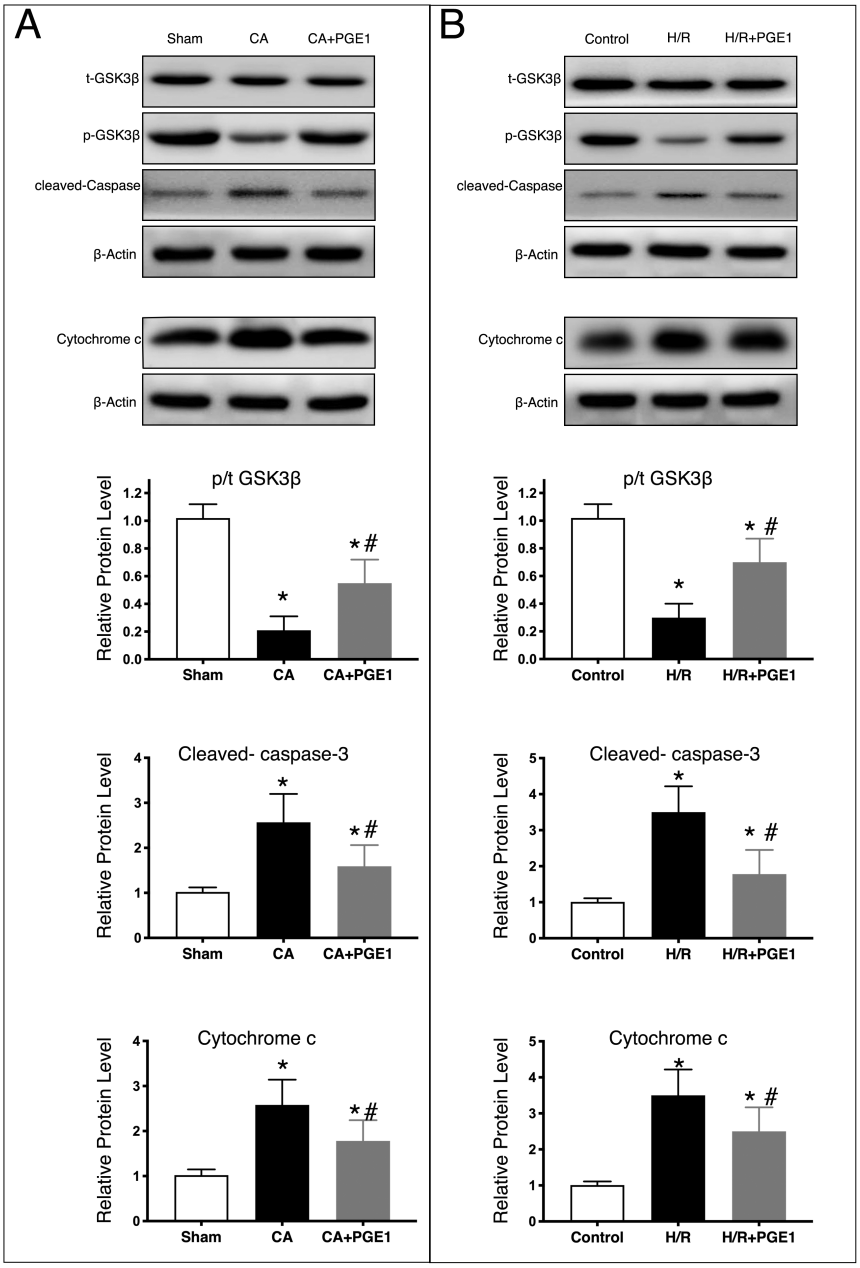

Figure 6

Effects of PGE1 on expression of GSK-3, cytochrome c and cleaved-Caspase3. (A): p-GSK3β, cytochrome c, cleaved-Caspase3 proteins expression in rats, #p<0.01 vs. sham group, *p<0.01 vs. CA group. (B): GSK3β, cytochrome c, cleaved-Caspase3 protein expression in H9ce cells. #p<0.01 vs. control group, *p<0.01 vs. H/R group.